THE JOURNAL OF PHYSICAL CHEMISTRY B LETTERS

2009, *113,* 16291–16295
Published on Web 10/20/2009

Quantum Coherence Enabled Determination of the Energy Landscape in Light-Harvesting Complex II

Tessa R. Calhoun,[†,‡] Naomi S. Ginsberg,[†,‡] Gabriela S. Schlau-Cohen,[†,‡] Yuan-Chung Cheng,[†,‡,||] Matteo Ballottari,[§] Roberto Bassi,[§] and Graham R. Fleming*[,†,‡]

Department of Chemistry and QB3 Institute, University of California, Berkeley, California 94720, Physical Biosciences Division, Lawrence Berkeley National Laboratory, Berkeley, California 94720, and Department of Biotechnology, University of Verona, 37134 Verona, Italy

Received: August 27, 2009; Revised Manuscript Received: September 29, 2009

The near-unity efficiency of energy transfer in photosynthesis makes photosynthetic light-harvesting complexes a promising avenue for developing new renewable energy technologies. Knowledge of the energy landscape of these complexes is essential in understanding their function, but its experimental determination has proven elusive. Here, the observation of quantum coherence using two-dimensional electronic spectroscopy is employed to directly measure the 14 lowest electronic energy levels in light-harvesting complex II (LHCII), the most abundant antenna complex in plants containing approximately 50% of the world's chlorophyll. We observe that the electronically excited states are relatively evenly distributed, highlighting an important design principle of photosynthetic complexes that explains the observed ultrafast intracomplex energy transfer in LHCII.

In the initial stages of photosynthesis, solar energy is absorbed by and transferred through intricate networks of pigment−protein complexes with unrivaled speed and efficiency. The key to understanding how these complexes function, and the proposed modulation of the function,[1−3] lies in the relationship between the spatial organization of their pigments and the resulting excited-state potential energy surfaces. In almost all photosynthetic complexes, however, the excitons composing this energy landscape are so closely spaced that they become indiscernible in the linear absorption spectrum, even at cryogenic temperatures. This spectral congestion has meant that assignment of electronic energy levels is indirect, because it is based on extensive modeling in combination with multiple forms of spectroscopy.[1,4]

In the study of photosynthetic complexes, much attention has recently been paid to the role of quantum coherences, coherent superpositions of excitons that can be prepared when a broad-band light pulse excites the system.[5−9] Quantum coherence in a photosynthetic system was first observed in the Fenna−Matthews−Olson complex[5,10] and has been discussed as an integral component of highly efficient photosynthetic light harvesting.[5−8,11] If we describe the evolution of these electronically excited complexes by the time progression of the density matrix for a two-level system

$$|\Psi(t)\rangle\langle\Psi(t)| = |a|^2|e_1\rangle\langle e_1| + |b|^2|e_2\rangle\langle e_2| + ab^*e^{-i(\omega_1-\omega_2)t}|e_1\rangle\langle e_2| + a^*be^{i(\omega_1-\omega_2)t}|e_2\rangle\langle e_1| \quad (1)$$

the first two terms, describing population elements, are stationary, while the final two terms, describing coherence elements, evolve with a phase factor associated with the energy difference between the two levels. Two-dimensional spectroscopy measures this phase evolution which manifests itself as an oscillation in the amplitude of the peaks in 2D spectra.[9,12] Therefore, while spectral broadening effects may prohibit resolution of individual excitons, each exciton contribution buried within a broad peak oscillates with a unique pattern. The excitons' characteristic beating frequencies, combined with the ability of two-dimensional spectroscopy to specifically probe coherence contributions to the signals, provide a method by which the individual excitons can be precisely located.

The 2D electronic spectroscopy experiment[13−16] and apparatus[10,15] have been described in detail elsewhere. Briefly, three broad-band pulses from a noncollinear optical parametric amplifier, separated by two time delays, coherence time (τ), and waiting time (T), are incident on the sample in a box geometry. The signal field proportional to the resulting third-order polarization is heterodyne-detected and spectrally resolved in a given phase-matched direction. The coherence time, τ, is scanned from negative to positive time at a fixed waiting time, and Fourier transformation along the τ axis produces a 2D spectrum. The 2D spectrum provides a map that correlates the excitation and emission frequencies of the sample; the peaks along the diagonal correspond to those in the linear absorption, and off-diagonal features, "cross peaks", arise from electronic coupling between pigments and energy transfer between excitons. Furthermore, excitonic quantum coherence manifests itself

* To whom correspondence should be addressed. Phone: (510) 643-2735. Fax: (510) 642-6340. E-mail: GRFleming@lbl.gov.
[†] University of California, Berkeley.
[‡] Lawrence Berkeley National Laboratory.
[§] University of Verona.
[||] Present address: Department of Chemistry, National Taiwan University, Taipei City 106, Taiwan.

10.1021/jp908300c CCC: $40.75

as oscillations in the amplitude of the diagonal and cross peaks as a function of T. In congested spectra where excitons are closely spaced energetically, cross peaks will appear near their diagonal counterparts. As a result, oscillations in the amplitude of cross peaks can interfere with those of the peaks directly on the diagonal, making it extremely difficult to isolate individual coherence contributions in conventional 2D spectra. Recently, we have shown that only diagonal signals arising from quantum coherences appear in nonrephasing 2D spectra, allowing them to be analyzed free from interference of beating cross peaks.[12] Nonrephasing spectra include data from only negative coherence time contributions, where the time ordering of the first two pulses is reversed.

Evolution of the diagonal cut of the nonrephasing 2D spectra as a function of waiting time, T, thus provides a means to specifically probe the coherent phase evolution of superpositions of excitons prepared by the first two laser pulses in the experiment. A Fourier transform with respect to T resolves the frequencies of the coherence oscillations to yield a power spectrum of these beat frequencies versus exciton energies. Each peak on this coherence power spectrum can be assigned specifically to a coherence density matrix element (eq 1). In an energetically disordered system, each exciton can participate in multiple coherences with other excitons in the system. This leads to a pattern of beat frequencies unique to each exciton whose peaks in the power spectrum line up along the same exciton energy, indicating the exciton's position and permitting direct measurement of the energy landscape. Furthermore, a coherent superposition of two excitons gives rise to a pair of "mirror peaks" that appear at the same beat frequency and the respective energies of the two contributing excitons, which can be useful in assigning excitons with low oscillator strength. If only one mirror peak is detected in the power spectrum, the location of the second exciton can be estimated from the energy of the first exciton and the beat frequency.

We have applied this technique to investigate coherence evolution of excitations in LHCII, the major light-harvesting complex in plants. The trimeric X-ray crystal structure of LHCII was determined at high resolution,[17,18] showing that each protein monomer contains 14 chlorophyll molecules with 2 spectral variants, 8 chlorophyll a (Chl a) molecules, producing an absorption band from 14 500 to 15 000 cm^{-1}, and 6 chlorophyll b (Chl b) molecules, giving rise to an absorption peak at 15 500 cm^{-1} (Figure 1). Even at 77 K, the 14 lowest-energy (Q_y) electronic transitions arising from the chlorophyll molecules cannot be distinguished in the linear absorption spectrum (Figure 1B). This congestion is extended to the 2D relaxation spectrum, shown in Figure 2A for $T = 250$ fs, where the diagonal features correspond to those in the linear absorption. Energy transfer from Chl b to Chl a as well as relaxation within the Chl a region can be seen in the 2D relaxation spectrum via strong cross peaks below the diagonal, while the negative features above the diagonal arise from excited-state absorption (ESA) to the large manifold of two-exciton states. The corresponding nonrephasing 2D spectrum in Figure 2B has characteristic "phase-twisted" line shapes[12,13] and comparatively enhanced cross peaks as the strong stationary signal along the diagonal from rephasing pathways has been removed. While the nonrephasing line shape has been shown to increase resolution along the diagonal,[19] it is clear in Figure 2B that this enhancement alone is not sufficient to isolate the 14 individual contributions to the diagonal signal.

To resolve the oscillations in spectral amplitude arising from electronic coherences in LHCII, spectra were collected for waiting times from 0 to 500 fs in 10 fs steps. Selected

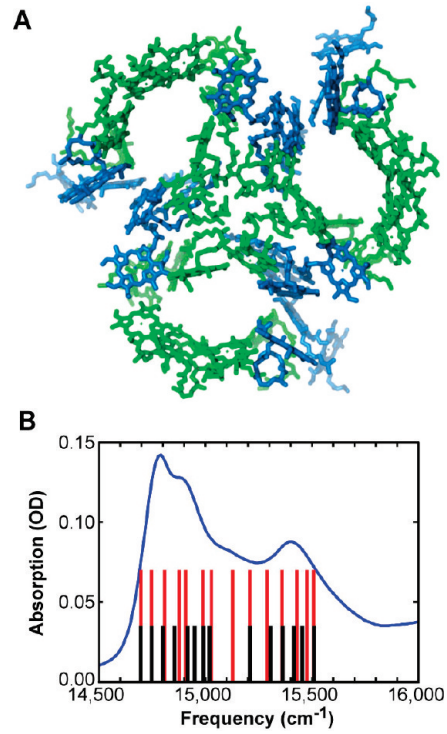

Figure 1. (A) Chlorophyll arrangement in LHCII trimer with Chl a and Chl b shown in green and blue, respectively. The phytyl chains have been omitted for clarity.[17] (B) Linear absorption spectrum of LHCII trimers at 77 K. Red sticks indicate the exciton energies determined in this experiment, while black sticks are previously predicted values.[1]

nonrephasing 2D spectra are shown in Figure S1 (Supporting Information), where the relative amplitudes of the diagonal features visibly oscillate, indicative of coherence quantum beating. Figure 2C shows the amplitude along the diagonal of the nonrephasing 2D spectra as a function of waiting time, where the exciton energy axis denotes the diagonal frequency in the 2D spectra. Quantum beating is clearly observed in both Chl a and b regions. As seen in other photosynthetic complexes,[5] the coherence is long-lived in LHCII, with the quantum beating lasting beyond the 500 fs scan of the experiment and beyond the lifetimes of many excitons in the system,[1] suggesting that this is a general phenomenon in photosynthetic systems. This result supports the speculation that evolution has designed these complexes to preserve coherence, a feat likely achieved through strongly correlated protein environments.[11,20−22] Recent studies suggest that such long-lived coherence is instrumental in facilitating extremely efficient energy transfer.[5−8]

Figure 3A shows the LHCII coherence power spectrum obtained by Fourier transforming the diagonal amplitude of nonrephasing 2D spectra (Figure 2C) along the waiting time axis. Clearly, the peaks in the power spectrum align vertically, indicating locations of the exciton levels. Figure 4A shows an expanded view of the Chl a region denoted by the box in Figure 3A. The circled peak with an exciton energy of 14 800 cm^{-1} and a beat frequency of 150 cm^{-1} has a distinct low-energy wing (arrow) that indicates the position of an exciton with slightly lower energy causing a slightly lower beat frequency peak. This feature illustrates how this experimental technique can utilize individual beat frequency patterns to separate energetically similar excitons. Furthermore, as the beat frequencies of the coherences experience relatively weak bath effects, simulation of the power spectrum presents us with the unique opportunity to directly access the system's electronic Hamil-

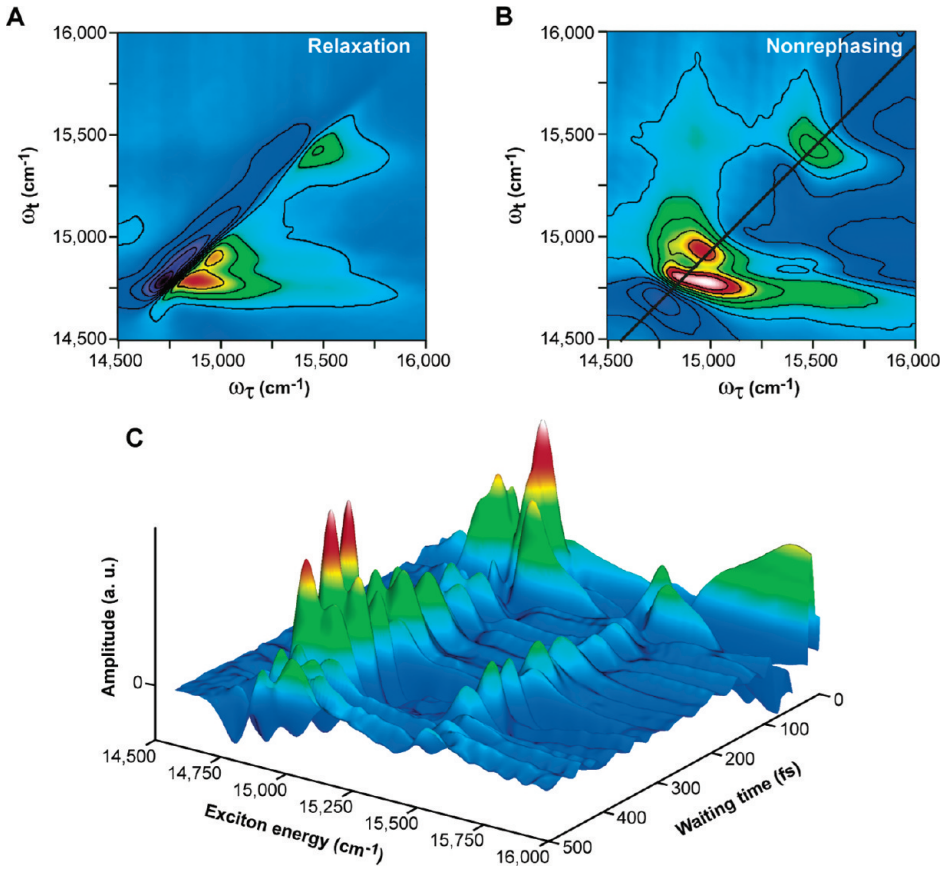

Figure 2. (A) The real part of a representative 2D relaxation spectrum for $T = 250$ fs. (B) The real part of the nonrephasing 2D spectrum for $T = 250$ fs. (C) The amplitude of the diagonal cut of the nonrephasing 2D spectra as a function of waiting time. For the purposes of presentation, a cubic spline interpolation connects the data points that were acquired in 10 fs increments. For (A−C), the amplitude increases from purple (negative) to white (positive).

tonian. Our initial comparison with the experimental data was done with the coherence power spectrum calculated from the Hamiltonian developed for a LHCII trimer by Novoderezhkin et al.[1] The comparison is shown in Table 1 and graphically in the Supporting Information. While there is considerable qualitative agreement between experiment and the model, there were significant differences in the exciton position and peak amplitude. Therefore, we developed a new model based on couplings calculated by Frähmcke and Walla[23] and site energies that were adjusted to give better agreement with the data. Details of both models can be found in the Supporting Information. Figure 3B displays the coherence power spectrum calculated by our new model; it is important to note that because Chl $b \rightarrow$ Chl a relaxation effects[24] are not included, features arising from coherences involving primarily Chl b excitations appear artificially stronger in the simulations. Figure 4B zooms in on the Chl a region for a detailed comparison to experiment, in which it can be seen that all of the features' positions and amplitudes are well reproduced. Clearly, simulation of the coherence power spectrum provides a stringent test for models of pigment−protein complexes, enabling better refinement of theoretical models.

Analysis of the entire experimental power spectrum yields the exciton energies in Table 1. Excitons 9 and 10 have very low oscillator strengths in the experimental data, and their positions were largely determined from several mirror peaks. This is consistent with previous modeling efforts in which excitons on the red edge of the Chl b band have been predicted to be "dark".[4] The most striking difference in Table 1 between the experiment and previous model is the higher energy positions of excitons 6−8, the three highest energy excitons in the Chl a region. Of specific interest is the location of exciton 8 shown by the peak at an exciton energy of 15 130 cm^{-1} and a beat frequency of ∼400 cm^{-1} in the experimental power spectrum (Figure 3A); this same region in the simulated spectrum from Novoderezhkin et al.[1] (Figure S2, Supporting Information) is devoid of any features. Exciton 8 is thus located in the intermediate region of the spectrum where no exicton had been predicted previously, yet it is almost exactly at the position of a weak shoulder on the blue edge of the Chl a linear absorption. This may explain why unique dynamics are observed in LHCII when pumping at this energy.[25]

The experimentally determined LHCII exciton energies reveal a reduction of the energetic gap between the Chl b and Chl a bands compared to previous assignments, resulting in a more evenly spaced energetic surface. This suggests that spacing between energy levels in LHCII may be tuned to match phonon frequencies of the surrounding proteins to optimize the efficiency of energy transfer since it is these vibrational modes that dissipate excess energy during exciton relaxation. The energy gap between Chl b and Chl a bands in LHCII was previously predicted[1] to be approximately 190 cm^{-1}, while studies of chlorophyll−protein complexes found that few protein vibrational modes in that region are strongly coupled to the chlorophylls' Q_y excited states.[26] The rate of energy transfer between Chl b and Chl a bands, however, has previously been observed to occur on a subpicosecond time scale with an extremely rapid 150−300 fs component.[25] While multivibrational quanta transitions are expected to play a large role in the slower interband relaxation rates,[27] this fastest rate is likely dominated by single quantum transitions requiring a smaller

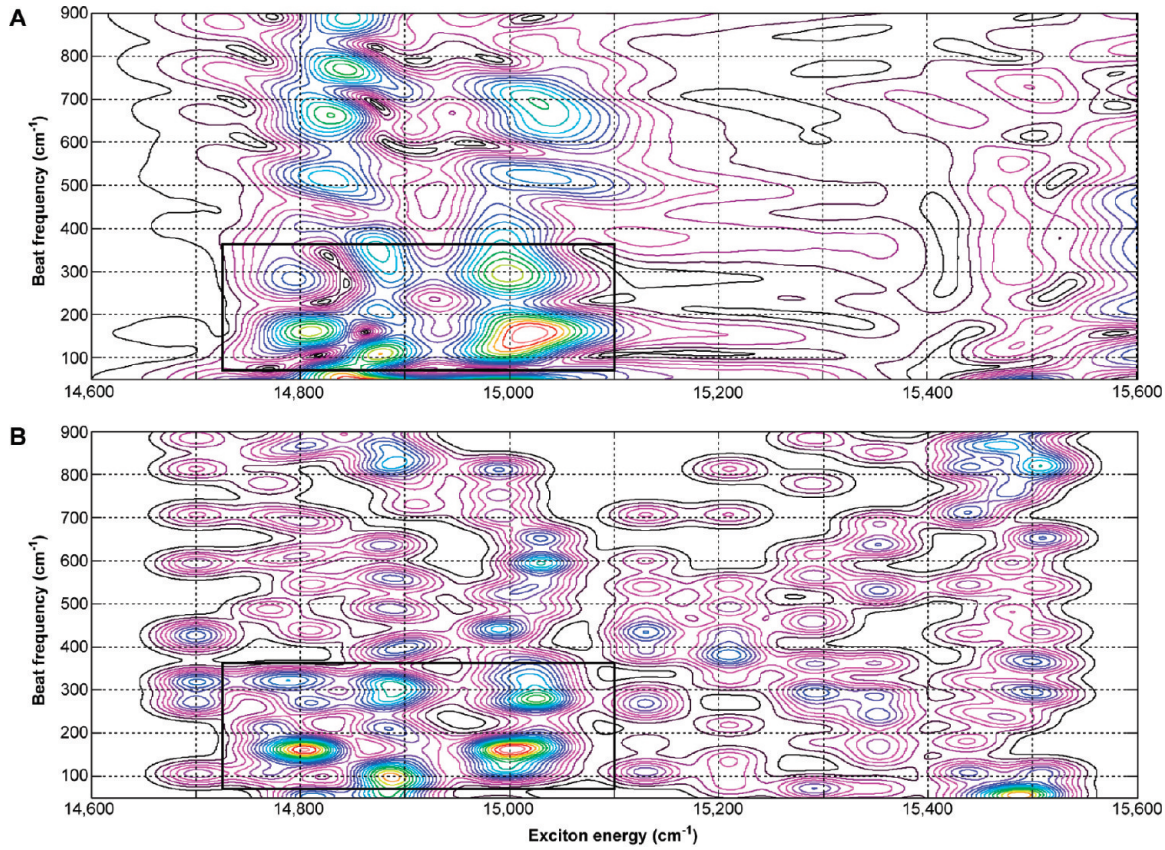

Figure 3. Power spectra of quantum beating in LHCII constructed from experimental 2D data (A) and theoretical simulations (B) as described in the text. The beat frequency axis begins at 50 cm^{-1} to remove the strong DC component, and contours are placed at 5% intervals. The boxes indicate the regions examined in detail in Figure 4.

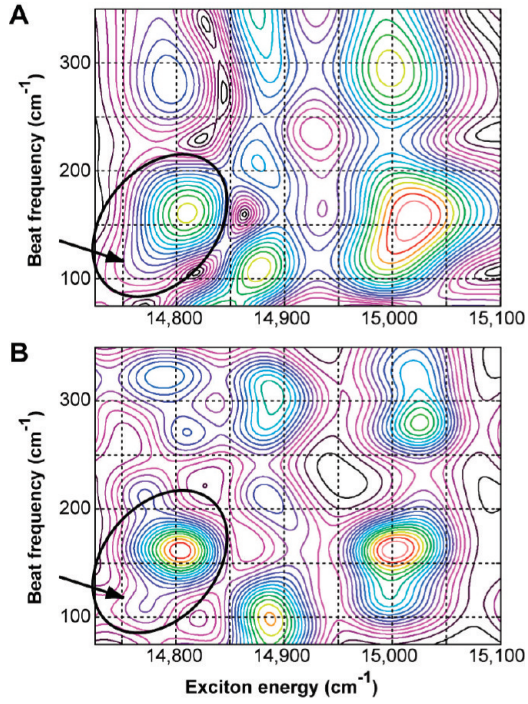

Figure 4. Zoomed-in region of the power spectra shown boxed in Figure 3. The circled peak and arrow highlight features discussed in the text.

energetic gap. The density of vibrational modes near 100 cm^{-1}, closer to the energetic gap found in this study, is more than twice as large as that for 190 cm,$^{-1}$ [26] thereby facilitating Chl *b* to Chl *a* energy transfer. The reduced spacing between Chl *a*/*b* bands revealed in this work could therefore explain the most rapid interband energy transfer in the LHCII.

TABLE 1: Exciton Energies Determined from the 2D Electronic Spectroscopy Experiment Compared with Those Calculated from Previous Models

exciton	experimental energy (cm^{-1})[a]	theoretical energy (cm^{-1})[b]
1	14700	14699
2	14770	14751
3	14810	14804
4	14880	14858
5	14910	14918
6	**14990**	14952
7	**15030**	14992
8	**15130**	15022
9	15210	15210
10	15290	15306
11	15360	15363
12	15430	15416
13	15480	15456
14	15510	15512

[a] Present work. Exciton energies over 30 cm^{-1} higher than theoretical predictions are highlighted in boldface. [b] From ref 1.

Two significant applications of the coherence power spectrum technique described here seem apparent. There is substantial evidence that photosynthetic complexes change their structural conformation, and hence their energy landscape, in vivo to create dramatic changes in their function, for example, allowing the same complex to transfer excitation efficiently in low light conditions and to dissipate excess energy in high light.[2,28] Application of this technique to structurally similar photosynthetic complexes that exhibit switchable functions, such as the photosystem II minor complexes,[3,28] should provide insight into

how nature has achieved this adaptive versatility. Second, the technique described here represents a significant step toward the determination of the full density matrix of molecular complexes, that is, quantum-state tomography.[29] Each of the peaks in Figure 3A corresponds directly to an individual off-diagonal element in the system's density matrix weighted by the appropriate dipole factors. If the dipole factors are known, such plots could be used to experimentally evaluate, for example, entanglement witnesses and determine the role of nonlocal behavior in photosynthetic light harvesting.

Acknowledgment. The authors thank Rienk van Grondelle for valuable discussions. This work was supported by the Director, Office of Science, Office of Basic Energy Sciences, of the U.S. Department of Energy under Contract DE-AC02-05CH11231 and the Division of Chemical Sciences, Geosciences, and Biosciences, Office of Basic Energy Sciences of the U.S. Department of Energy through Grant DE-AC03-76SF000098 (at LBNL and UC Berkeley) and by the Italian Basic Research Foundation Contracts FIRB RBLA0345SF002 (Solanacee) and FISR IDROBIO (University of Verona). N.S.G. thanks the LBNL Glenn T. Seaborg postdoctoral fellowship for support.

Supporting Information Available: Details about sample preparation, experimental conditions, and simulations; selected nonrephasing 2D spectra exhibiting quantum beating of diagonal features; and a theoretical coherence power spectrum calculated from the LHCII trimer Hamiltonian by Novoderezhkin et al.[1] This material is available free of charge via the Internet at http://pubs.acs.org.

References and Notes

(1) Novoderezhkin, V. I.; Palacios, M. A.; van Amerongen, H.; van Grondelle, R. *J. Phys. Chem. B* **2005**, *109*, 10493.

(2) Ruban, A. V.; Berera, R.; Ilioaia, C.; van Stokkum, I. H. M.; Kennis, J. T. M.; Pascal, A. A.; van Amerongen, H.; Robert, B.; Horton, P.; van Grondelle, R. *Nature* **2007**, *450*, 575.

(3) Ahn, T. K.; Avenson, T. J.; Ballottari, M.; Cheng, Y.-C.; Niyogi, K. K.; Bassi, R.; Fleming, G. R. *Science* **2008**, *320*, 794.

(4) Linnanto, J.; Martiskainen, J.; Lehtovuori, V.; Ihalainen, J.; Kananavicius, R.; Barbato, R.; Korppi-Tommola, J. *Photosynth. Res.* **2006**, *87*, 267.

(5) Engel, G. S.; Calhoun, T. R.; Read, E. L.; T.K., A.; Mancal, T.; Chung, Y.-C.; Blankenship, R. E.; Fleming, G. R. *Nature* **2006**, *446*, 782.

(6) Plenio, M. B.; Huelga, S. F. *New J. Phys.* **2008**, *10*, 113019.

(7) Olaya-Castro, A.; Lee, C. F.; Olsen, F. F.; Johnson, N. F. *Phys. Rev. B* **2008**, *78*, 7.

(8) Mohseni, M.; Rebentrost, P.; Lloyd, S.; Aspuru-Guzik, A. *J. Chem. Phys.* **2008**, *129*, 174106.

(9) Pisliakov, A. V.; Mancal, T.; Fleming, G. R. *J. Chem. Phys.* **2006**, *124*, 234505.

(10) Brixner, T.; Stenger, J.; Vaswani, H. M.; Cho, M.; Blankenship, R. E.; Fleming, G. R. *Nature* **2005**, *434*, 625.

(11) Lee, H.; Cheng, Y. C.; Fleming, G. R. *Science* **2007**, *316*, 1462.

(12) Cheng, Y. C.; Fleming, G. R. *J. Phys. Chem. A* **2008**, *112*, 4254.

(13) Hybl, J. D.; Ferro, A. A.; Jonas, D. M. *J. Chem. Phys.* **2001**, *115*, 6606.

(14) Jonas, D. M. *Annu. Rev. Phys. Chem.* **2003**, *54*, 425.

(15) Brixner, T.; Manĉal, T.; Stiopkin, I. V.; Fleming, G. R. *J. Chem. Phys.* **2004**, *121*, 4221.

(16) Cowan, M. L.; Ogilvie, J. P.; Miller, R. J. D. *Chem. Phys. Lett.* **2004**, *386*, 184.

(17) Liu, Z. F.; Yan, H. C.; Wang, K. B.; Kuang, T. Y.; Zhang, J. P.; Gui, L. L.; An, X. M.; Chang, W. R. *Nature* **2004**, *428*, 287.

(18) Standfuss, J.; van Scheltinga, A. C. T.; Lamborghini, M.; Kuhlbrandt, W. *EMBO J.* **2005**, *24*, 919.

(19) Ge, N. H.; Zanni, M. T.; Hochstrasser, R. M. *J. Phys. Chem. A* **2002**, *106*, 962.

(20) Muh, F.; Madjet, M. E. A.; Adolphs, J.; Abdurahman, A.; Rabenstein, B.; Ishikita, H.; Knapp, E. W.; Renger, T. *Proc. Natl. Acad. Sci. U.S.A.* **2007**, *104*, 16862.

(21) Yu, Z. G.; Berding, M. A.; Haobin, W. *Phys. Rev. E* **2008**, *78*, 050902.

(22) Collini, E.; Scholes, G. D. *Science* **2009**, *323*, 369.

(23) Frahmcke, J. S.; Walla, P. J. *Chem. Phys. Lett.* **2006**, *430*, 397.

(24) Ishizaki, A.; Fleming, G. R. *J. Chem. Phys.* **2009**, *130*, 23411.

(25) van Grondelle, R.; Novoderezhkin, V. I. *Phys. Chem. Chem. Phys.* **2006**, *8*, 793.

(26) Renger, T.; Marcus, R. A. *J. Chem. Phys.* **2002**, *116*, 9997.

(27) Renger, T.; Trostmann, I.; Theiss, C.; Madjet, M. E.; Richter, M.; Paulsen, H.; Eichler, H. J.; Knorr, A.; Renger, G. *J. Phys. Chem. B* **2007**, *111*, 10487.

(28) Dall'Osto, L.; Caffarri, S.; Bassi, R. *Plant Cell* **2005**, *17*, 1217.

(29) Nielsen, M. A.; Chuang, I. L. *Quantum Computation and Quantum Information*; Cambridge University Press: Cambridge, U.K., 2000.

JP908300C